This full text paper was peer-reviewed at the direction of IEEE Instrumentation and Measurement Society prior to the acceptance and publication.

Pressure sensors used as bioimpedance plantar electrodes: a feasibility study

Isabel Morales
Núcleo de Ingeniería Biomédica
Universidad de la República
Montevideo, Uruguay
imorales@fing.edu.uy

Rafael González-Landaeta
Ingeniería Eléctrica y Computación
Univ. Autónoma de Ciudad Juárez
Chihuahua, México
rafael.gonzalez@uacj.mx

Franco Simini
Núcleo de Ingeniería Biomédica
Universidad de la República
Montevideo, Uruguay
simini@fing.edu.uy

Abstract*—Diabetic Foot Ulcers are ominous consequence of Diabetic Foot. Only general preventive guidelines are available, and ulcers happen with no previous notice. To develop a multidimensional ulcer opening warning device: temperature, pressure, humidity and friction are usually considered. We use standard flexible Force Sensing Resistors FSR 402 to detect not only plantar pressure, but also plantar bioimpedance. Since FSR includes conductive electrodes covered by polymer films, the interface with the subject can be considered a capacitive electrode. A special bioimpedance detection circuit is required to inject current using two homologous FSR 402 contacts and measuring the resulting voltage from the other two contacts available. This circuit is able to detect the cardiac activity from the foot sole. For the first time, pressure sensors are used as bioimpedance electrodes.*

Keywords— diabetic foot ulcer, pressure sensor, bioimpedance, impedance plethysmography, plantar electrodes, wearable device

I. Introduction

Diabetes Mellitus (DM) is a growing public health concern worldwide [1] and one of its several complex complications is diabetic foot disease. In most cases diabetic patients have similar induced pathologies such as sustained hyper-glycaemia, diabetic peripheral neuropathy and peripheral artery disease. Indeed, the process that leads to a diabetic foot ulcer (DFU) is a consequence of two or more of these risk factors present for a given person [2].

Self-care education and self -care management are the only preventive measures available nowadays to prevent DFUs. The International Working Group on the Diabetic Foot (IWGDF) publishes a Risk Stratification System to be used during assessment and follow-up, based on prospective risk factor and early signs of foot ulceration [2].

The identification of the *at-risk foot* and regular inspection as well as foot examination includes such objective and subjective information as plantar pressure, vibration perception and vascular status. Once the DFU is diagnosed, thermography, plantar pressure and temperature measurements are used to monitor it from medical visit to next one. The follow-up consists mostly of wound healing, footwear solutions and pressure offloading [3] [4].

Thermography can provide real-time physiologic imaging and can help to identify a small rise in temperature which is considered an early sign of a DFU [5]. The emitted energy from a living tissue is usually interpreted as a color-coded image. It allows estimating the temperature distribution of an area, regardless of its shape [6]. This evaluation can only be performed on the naked foot in the physician's office.

The assessment of *at-risk foot* never involves plantar pressure by itself because of its poor specificity. High plantar pressure increases the risk of developing DFUs and managing its peak pressure is therefore important. Pressure sensors continuously measure plantar pressure and could provide feedback to the peripheral neuropathy patient [3]. Current research focuses on the determination of pressure thresholds to predict high DFU risk [7]. This risk is assessed during a medical visit and without the dynamic functional component of gait [8] .

Nowadays, various laboratory plantar sensing systems are commercially available. Plantar pressure can be measured by footprint infrared imaging scan, force plate, or pressure insoles. Pressure insoles can be designed from pressure-sensitive materials based on either capacitive sensing or piezoelectric/piezoresistive sensing [9].

The skin temperature distribution and its pressure related pattern are conjunctively being studied [5]. From a pressure ulcer prevention research perspective, the temperature distribution may be linked to concurrent soft tissue deformation. Kottner supports that if microclimate around the foot is preserved, no pressure ulcer should happen [10].

To monitor diabetic foot health and to provide a better control over any imminent foot lesion, a review of the literature suggests a clear demand of an early alert device. We have thus defined, as a possible solution, an inexpensive wearable device with smart sensors, named DIAPODAL.

Our goal is to alert the person in time so that a low level of ulcer risk can be kept. This would be accomplished by continuous assessment of skin parameters such as bioimpedance, vascular status, humidity, pressure, temperature, friction, all considered measurable dimensions of DFU risk level. By combining these parameters DIAPODAL should calculate a pre ulcerative score.

Bioimpedance is capable of long-term monitoring of skin integrity and of acute wound healing [11]. Furthermore, an appropriate selection of measurement frequency can unveil characteristics of different skin layers, tissue depths and vascular status. However, there are no explicit studies showing bioimpedance as a real time DFU prevention tool instead of the usual passive monitoring during medical visits.

Impedance plethysmography (IPG) is a technique to detect variations in electrical impedance related to changes in volume in some body tissues. It is namely used to study lower limbs to determine volume changes due to blood flow [12]. A four-electrode array can be placed in a single foot to detect heart beat [13]. Beat-to-beat heart signals are thus obtained, to estimate, for example, the heart rate of a subject [7].

This paper aims to study the feasibility of using a standard pressure sensor, with an appropriate setup, as a plantar bioimpedance electrode. To validate such use, we suggest processing the plantar bioimpedance signal by IPG. If the processed signal performs correctly as an impedance plethysmograph following closely a standard heart rate

978-1-6654-1914-7/21/$31.00 ©2021 IEEE

monitor, the pressure sensor will have performed correctly as a couple of bioimpedance electrodes.

The present study is a first approximation to this approach. The goal set here is the design of a circuit to measure foot bioimpedance using standard force sensing resistors sensors. Data from a healthy subject are considered during trials for IPG signals with pressure sensors, Ag-AgCl ECG electrodes and capacitive aluminum foil pads.

II. Force Pressure Sensors

Plantar pressure is an important indicator of foot health condition and gait patterns [8]. Theory has demonstrated a great correlation degree between the DFUs and higher plantar loads due to diabetic neuropathy [14].

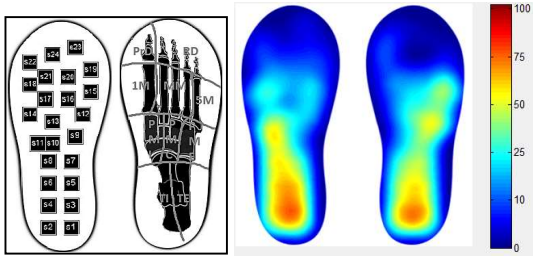

Figure 1. Twenty-four force sensing resistors FSR 402. Static plantar pressure distributed measurements after Gaussian low pass filter.

Previous work on foot pressure sensing was done using model FSR 402 [15]. A 24-sensor insole gave accurate results grouped in 10 anatomical areas for clinical analysis, both static and dynamic. Figure 1 shows a static image of foot pressure during standing position. Figure 2 shows the distribution of pressures in an arbitrary order of foot areas from Toe Tip (Pdr Spanish acronym for ToT) to External Heel (TE Spanish acronym for EH).

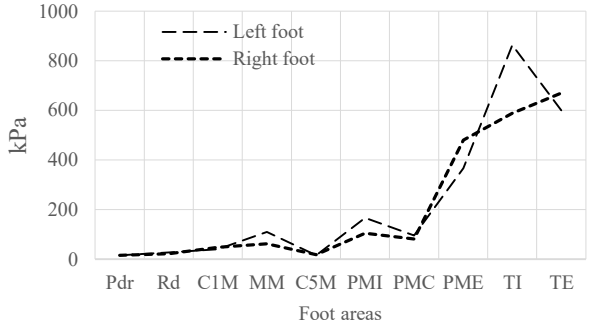

Figure 2. Pressure as measured in ten-foot sole areas during static stand.

A. Selecting a pressure sensor

Current studies are exploring different pressure sensor instrumentation. Table 1 shows the most representative for plantar pressure follow-up. Analog pressure sensors are either variable resistor, potentiometers or capacitive.

Piezo elements are useful to detect vibration or knocks while force sensing resistor have a wider measurement range of applications.

B. Force Sensing Resistor Specifications

A Force Sensing Resistor (FSR) is a variable resistor that provides a change of its electrical resistance as a function of the force applied on its active area [16]. As the force increases the electrical resistance decreases in a nonlinear way.

TABLE I. Analog Pressure Sensors Characteristics

Model	*Sensing area diameter x thickness*	*Shape*	*Pressure Min – Max*	*Materials*	*Price USD*
FSR 402	12.70 mm 0.20 mm	Circular	(0.1 to 10) kg	Polymer	7
Flex 2.2"	95.25 mm 0.43 mm	Rectangular	(10 – 70) kΩ (0°- 90°) angle	Polymer	9
Piezoelectric	12.00 mm 0.22 mm	Circular	8.0 nF ± 30% [1 kHz]	Brass	1.5
Piezocapacitive	0.10 mm 0.22 mm	Square	(0 to 800) kPa	Graphene	No data

FSR can be fabricated in various sizes, as Table 1 shows, a FSR 402 has a 10 kg maximum load response in an active area of 113 mm^2. Moreover, its resistance range is a good option for load pressure acquisition of a foot. A previous application was tailored as described in Figure 1. FSR can be bought with two solder tabs (Figure 3). Contacts that are stapled through the flexible substrate to connect the semi-conductive material [16]. Allows an easy and non-invasive integration into a sole because it is made of a flexible two polymer thick film (PTF) layer (0.20 mm) that allows the conductive pattern [17].

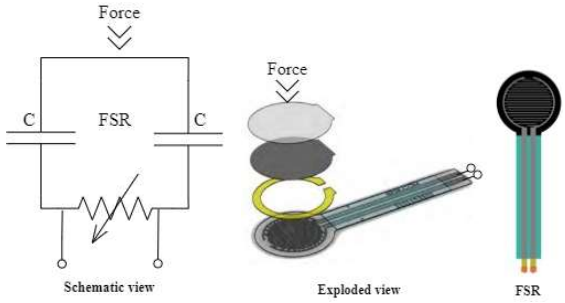

Figure 3 – Pressure force resistance sensor FSR 402. From left to right: proposed schematic, exploded view (first to fourth layer from top to bottom) and plantar view. Adapted from commercial material by Interlink [16].

The feasibility of using FSR pressure sensors as bioimpedance plantar electrodes relies on the four layers composition of the sensor. First and third layers work as insulators, second as top substrate and the fourth as conductive bottom substrate. The top substrate contains interdigitating conductive electrodes and the bottom a semiconductive polymer [17]. Thus, it could operate as capacitive electrode.

Figure 3 shows the proposed schematic view with an exploded view of the four FSR layers. This analysis helps understand the utilization of this sensor as a capacitive electrode.

III. Simulation

Bioimpedance applications use different types of electrodes, such as dry electrodes or capacitive electrodes [13]. Figure 4 shows the analogue tetrapolar configuration as used in bioimpedance with conventional electrodes.

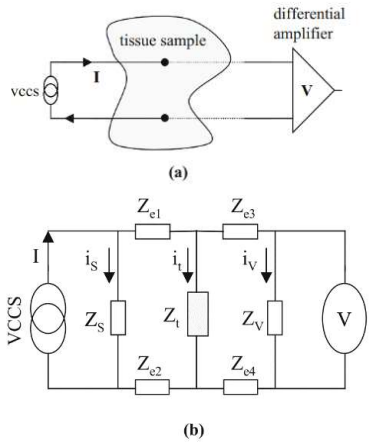

Figure 4 – (a) symbolic and (b) circuit representations of tetrapolar configurations to measure bioimpedance. Taken with permission from Bertemes-Filho and Simini [18] .

A. Original FSR configuration for bioimpedance

FSR are passive sensors made of material properties of polymers that could allow us to modify its function. By adding a combination of two sensors, such as shown in Figure 4, we could obtain plantar bioimpedance values, reaching comparable values to those obtain with conventional capacitive electrodes. For this reason, standard FSR sensors, originally designed for force sensing applications, could be applied. We have thus, the potential to obtain a simpler and lower cost sensor system for DFUs prevention.

We chose to use the homologous tabs of two FSR as current injection electrodes and the other two tabs as voltage measurement pair, Figure 5.

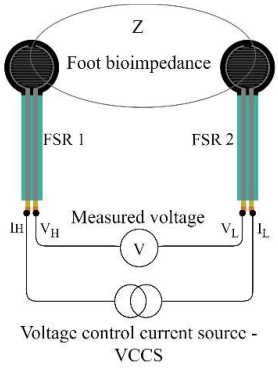

Figure 5 – Original configuration of two FSR 402 pressure sensors used also for bioimpedance measurement.

The FSR is usually modelled as a resistance in parallel with a single capacitance. That capacitance is assumed as the unique capacitance of the entire conductive part. Nonetheless, as show in Figure 3, FSR is modelled with two capacitances. In this sense, we present a tetrapolar configuration model for foot bioimpedance measurements, Figure 6.

Each FSR includes a variable resistance, the two extremities of which can be assumed to have a capacitive coupling with the underlying foot. This arrangement follows the configuration shown in Figure 4 which is a complete tetrapolar bioimpedance measurement circuit. For bioimpedance application, this module is more accurate than the single capacitor equivalent circuit suggested by Paredes-Madrid [20].

We consider each initial part of the FSR as a conductive electrode which constitutes a capacitive electrode. When working in a tetrapolar way, with four capacitors, the contribution of these impedances is reduced and then the resistance changes are more evident. The simulation demonstrates the essence of this analysis.

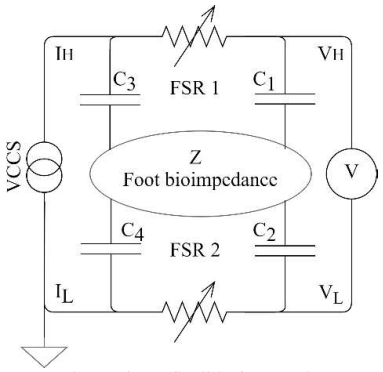

Figure 6 –. Suggested use of two flexible force resistor pressure sensors as bioimpedance electrodes. Each pressure sensor has two conductive contacts FSR 402.

B. Simulation results

We have performed a simulation using LTSPICE. Injected current was simulated as 1 mA at variable sinusoidal freqcuencies. Capacitance was set at 1 nF for both capacitors connected to each end of the sensors, C_1 and C_3 for FSR_1 and C_2 and C_4 for FSR_2. As a pressure sensor, when the foot loads an FSR, its resistance decreases tending to "short circuit" the bioimpedance layout. For this reason to overcome this difficulty one should implement the measurement of bioimpedance when the foot is in the air.

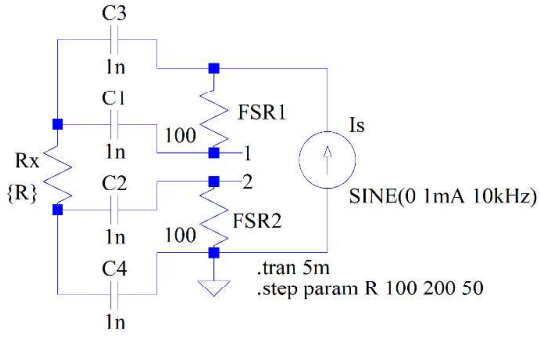

Figure 7 – Four–capacitor model simulation schematic.

The four-capacitor model of Figure 7 allows us to vary the resistance in steps of 50 Ω starting from 100 Ω to 200 Ω with resulting changes in impedance. We have repeated the same simulation for 10 kHz, 500 kHz and 1Mhz.

The simulation shows that with frequencies of 10kHz, capacitors encounter high impedance which implies that all current flows through the FSR resistance. Therefore, very little current goes to Rx, and therefore voltage changes to determine foot bioimpedance will be very small. However, at 1MHz of current excitation, there is a variation of

approximately 15% between resistance changes on contact 1 and 2 of Figure 7.

Figure 8– Voltage output of impedance measurement, contact 1&2 of Figure 7. 10 kHz, 1mA simulation parameters.

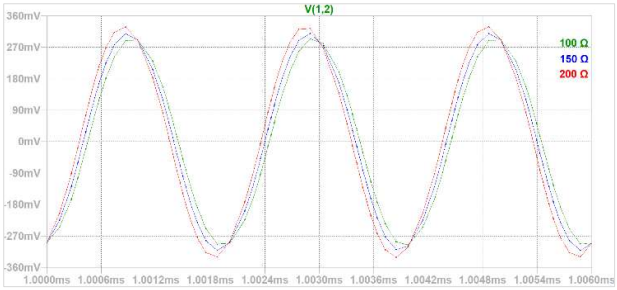

Figure 9– Voltage output of impedance measurement, contact 1&2 of Figure 7. 500 kHz, 1mA simulation parameters.

Figure 10– Voltage output of impedance measurement, contact 1&2 of Figure 7. 1 MHz, 1mA simulation parameters.

Figure 8 shows a 10 kHz frequency current simulation which resistance variations entailed no significant changes in voltage output. Figure 9 shows a 500 kHz simulation with resistance changes up to 5% phase-shifts in voltage amplitude. Finally, Figure 10 shows a 1MHz simulation which results into variations of up to 15% changes in voltage amplitude for 100 Ω, 150 Ω and 200 Ω respectively.

IV. Experimental Setup

Bioimpedance techniques are based on the injection into a tissue of an alternating electric current of low intensity [10].

A. Block diagram

Figure 11 shows the block diagram of the proposed system to detect the IPG using FSR. The system comprises a current source controlled by voltage, an ac coupled amplifier to acquire differential modulated signals because of blood flow, a single-ended synchronous demodulator filters and finally, as recommended, an extra gain-filter processing.

1) Voltage contolled current source - VCCS

An OPA27 differential amplifier is configured to deliver a Modified Howland current source to deliver a low intensity high-frequency ac current controlled by a 10 kHz sinusoidal signal with an amplitude of 1Vrms, delivered by a function generator.

A stable high-frequency current source is necessary for a wide variety of load impedance. Thus, to ensure that the intensity of the delivered current remains stable, regardless of the load impedance that is connected to the source output, a very high output impedance is needed. For this, the Modified Howland current source must be implemented with low tolerance resistors. The output of the voltage-controlled source VCCS us connected to a coupling capacitor to protect the volunteer from dc currents.

2) Acquisition stage

This stage detects response of injecting a low intensity high frequency current to the tissue. The signal obtained is an amplitude modulated signal that comprises the impedance of the non-pulsatile tissues and the changes of the impedance due to the pulsatile flow in larger arteries. The magnitude of the former is a thousand times higher than the latter.

The acquisition stage requires a careful selection of the input resistance to reduce loading errors.

3) Synchronous demodulator

Demodulation restores the original signal after conditioning the signal at high frequencies. Amplitude modulation is the product of itself with a modulating signal (10 kHz). The demodulation process involves the amplitude modulated signal being multiplied by a reference signal at the same frequency and phase as the carrier signal.

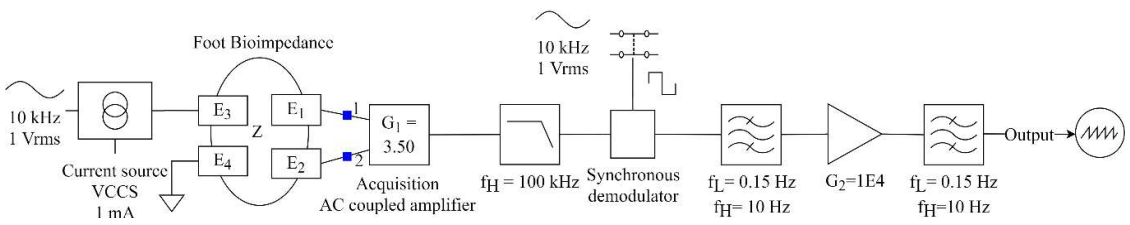

Figure 11 – Impedance plethysmography (IPG) foot bioimpedance block diagram. Contacts 1&2 are the same as contacts 1&2 of Figure 6.

4) Output stage

Following the demodulator, a filtering stage to restore the baseline and eliminate the DC offset voltage. Bandwidth is limited to 10 Hz. This value is twice the frequency of the heart signal. In addition, it limits noise and high-frequency components. The demodulation process attenuates the signal of interest. Then it is important to adapt the output amplitude.

B. *Impedance plethysmography measurement*

Impedance plethysmography (IPG) allows to measure cardiac activity by means of bioimpedance variations. Bioimpedance can be conducted by either two-electrode or four-electrode methods. In our case, current entries to specific plantar bioimpedance contacts.

Figure 11 shows a four-electrode IPG configuration: E1&E2 for voltage measurement and E3&E4 for current injection. The choice of the injection pair and the voltage measurement pair is based on usual tetrapolar considerations. Current lines run through the tissue and voltage is measured between two intermediate points where these lines are parallel.

C. *Measurement of volunteer foot bioimpedance*

The study was carried out in accordance with the guidelines approved by the University Ethics Committee of the Hospital de Clínicas, Uruguay. A healthy volunteer agreed to be part of the present research and signed the informed consent.

For first trials, we tested the system with 1) Ag-AgCl ECG electrodes placed side by side on lateral malleolus, 2) foil aluminum pads (handcraft electrodes of 4 cm^2) in both shoe soles and 3) FSR sensors in both shoe soles.

Figure 12 shows a cardiac signal of approximately 72 bpm obtained with the circuit of Figure 11. Since the signal was acquired using Ag-AgCl electrodes, the amplitude is in the range of 1.00 V. The baseline shows electrical noise or electromagnetic interference.

Figure 13 shows the signal from aluminum pads below the foot inside the shoe. Being a dry electrode, the amplitude is larger than the Ag-AgCl case. The cardiac rate is here 88 bpm of the same volunteer at some other time. With dry electrodes current paths are longer and run through more blood vessels. Noise and interference are similar to Figure 12.

Figure 14 shows the signal using FSRs as bioimpedance electrodes. The signal incudes several movement artifacts. The red circles feature cardiac activity at 72 bpm. Confirming the simulation, cardiac signal amplitude could increase with higher input frequency currents. Notice that injected current cannot be increased above the maximum value of safety standards. A new *Acquisition Stage* design of the circuit of Figure 11 may have to be optimized. The signal acquired and its similarity with signals obtained with other electrodes allows us to infer that FSRs can be used as electrodes to detect IPG.

To complete the implementation of the IPG system it is important to recognize and to understand the origin of the noise and electromagnetic interference. Thus, as future work, we must acquire the IPG signal with contact area of FSRs and compared it to conventional electrodes. Also, further analysis must be done with frequencies above 10kHz since simulations suggest those improvements for a better signal acquisition with FSRs. The feasibility is nevertheless confirmed at a primary level of evidence, both simulations and first measurements.

Future work includes the evaluation of the effect of increasing frequency on the IPG signal. Also, the origin of electromagnetic interferences and electrical noise to design appropriate neutralizations for a better signal.

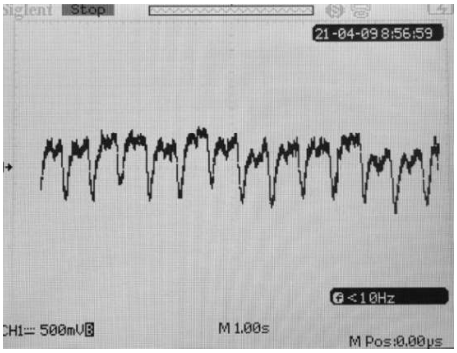

Figure 12 – IPG bioimpedance voltage measured with Ag-AgCl ECG electrodes. E1-E3 and E2-E4 placed on two points of lateral malleolus of both legs. System of Figure 11 was used.

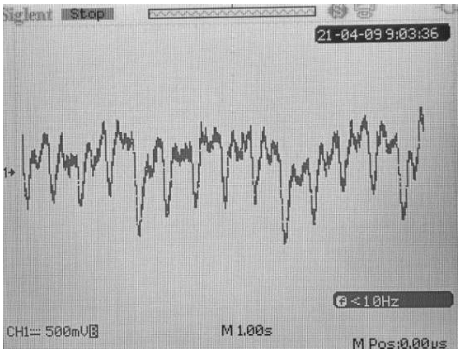

Figure 13 – IPG bioimpedance voltage measured with aluminum pads. E1-E3 and E2-E4 placed on shoe soles. System of Figure 11 was used.

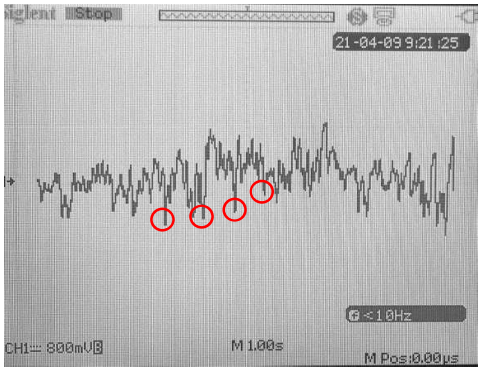

Figure 14– IPG bioimpedance voltage measured with FSR sensors. FSR_1 and FSR_2 on shoe soles with the circuit of Figure 11.

V. Discusion and conclusions

In this paper we have suggested the use of a FSR sensor as a bioimpedance measurement element. The bioimpedance set up was modelled as a tetrapolar configuration where each sensor contributes with two contacts. Each one represents a capacitive interface to the subject.

The results obtained here make feasible the fact to use pressure sensors as electrodes for bioimpedance measurements which simplifies the development of a wearable device to alert patients of an imminent DFU.

Adding different variables to describe the physical and physiological characteristics of the foot at any given time, we intend to present a comprehensive device to warn the user to stop walking and to keep at a low level the risk of DFU opening. Such a device will be for the first time available for diabetic persons.

As a feasibility study, the present contribution consists of a successful simulation along with an electronic point of view validated by experiments. The frequency of 10 kHz stems from practical electronic feasibility with limited noise compared to higher frequencies. There is a clear dependence on the frequency. This requires more mathematical analysis in the circuit model, but with the present simulations the proposal appears feasible. Additionally, we have reported the behavior of a real circuit on a healthy volunteer.

Acknowledgment

The authors acknowledge here the contributions made by Karina Quinteros who took part in the discussions on diabetic foot management from her podiatry point of view. Thanks are given to Profesor Beatriz Mendoza, Pablo Orellano and Mariana Risso from Department of Endocrinology, Hospital de Clínicas, Uruguay for useful comments and motivation.

A special acknowledgement is expressed to Professors Joaquim Gabriel and Arcelina Marques from Faculdade de Engenharia da Universidade do Porto and Instituto Superior de Engenharia do Porto, Portugal, for motivation and methodology.

References

[1] S. El-Sappagh, F. Ali, S. El-Masri, K. Kim, A. Ali, and K. S. Kwak, "Mobile Health Technologies for Diabetes Mellitus: Current State and Future Challenges," *IEEE Access*, vol. 7, no. e, pp. 21917–21947, 2019.

[2] J. Apelqvist, K. Bakker, W. H. van Houtum, N. C. Schaper, and International Working Group on the Diabetic Foot (IWGDF) Editorial Board, "Practical guidelines on the management and prevention of the diabetic foot: based upon the International Consensus on the Diabetic Foot (2007) Prepared by the International Working Group on the Diabetic Foot.," *Diabetes. Metab. Res. Rev.*, vol. 24 Suppl 1, pp. S181-7.

[3] S. A. Bus, "Innovations in plantar pressure and foot temperature measurements in diabetes," *Diabetes. Metab. Res. Rev.*, vol. 32, no. 1, pp. 221–226, Jan. 2016.

[4] A. Seixas *et al.*, "Skin temperature of the foot: Reliability of infrared image analysis based in the angiosome concept," *Infrared Phys. Technol.*, vol. 92, no. June, pp. 402–408, 2018.

[5] R. Vardasca, L. Vaz, C. Magalhaes, A. Seixas, and J. Mendes, "Towards the Diabetic Foot Ulcers Classification with Infrared Thermal Images," *14th Quant. InfraRed Thermogr. Conf.*, pp. 1–4, 2018.

[6] S. L. Bennett, R. Goubran, and F. Knoefel, "Long term monitoring of a pressure ulcer risk patient using thermal images," *Proc. Annu. Int. Conf. IEEE Eng. Med. Biol. Soc. EMBS*, pp. 1461–1464, 2017.

[7] B. Najafi, H. Mohseni, G. S. Grewal, T. K. Talal, R. A. Menzies, and D. G. Armstrong, "An Optical-Fiber-Based Smart Textile (Smart Socks) to Manage Biomechanical Risk Factors Associated with Diabetic Foot Amputation," *J. Diabetes Sci. Technol.*, vol. 11, no. 4, pp. 668–677, 2017.

[8] P. R. Cavanagh and J. S. Ulbrecht, "Clinical plantar pressure measurement in diabetes: rationale and methodology," *Foot*, vol. 4, no. 3, pp. 123–135, 1994.

[9] C. Lou *et al.*, "A graphene-based flexible pressure sensor with applications to plantar pressure measurement and gait analysis," *Materials (Basel).*, vol. 10, no. 9, 2017.

[10] J. Kottner, J. Black, E. Call, A. Gefen, and N. Santamaria, "Microclimate: A critical review in the context of pressure ulcer prevention," *Clin. Biomech.*, vol. 59, no. March, pp. 62–70, 2018.

[11] A. Kekonen, M. Bergelin, M. Johansson, N. K. Joon, J. Bobacka, and J. Viik, "Bioimpedance sensor array for long-term monitoring of wound healing from beneath the primary dressings and controlled formation of h2o2 using low-intensity direct current," *Sensors (Switzerland)*, vol. 19, no. 11, 2019.

[12] D. H. Díaz, Ó. Casas, R. Pallas-areny, and A. M. System, "Measurements in a Weighing Scale," *Power*, pp. 6489–6492, 2010.

[13] R. González-Landaeta, O. Casas, and R. Pallàs-Areny, "Heart rate detection from plantar bioimpedance measurements," *IEEE Trans. Biomed. Eng.*, vol. 55, no. 3, pp. 1163–1167, 2008.

[14] G. Rescio, A. Leone, L. Francioso, and P. Siciliano, "Sensorized Insole for Diabetic Foot Monitoring," *Proceedings*, vol. 2, no. 13, p. 860, 2018.

[15] I. Morales, "Development of an Electronic System for Static and Dynamic Analysis of Plantar Pressure," Universidad del Valle, 2011.

[16] I. Electronics, "FSR ® 400 Series Data Sheet Human - Machine Interface Solutions for a Connected World FSR ® 400 Series Data Sheet," 2015.

[17] S. I. Yaniger, "Force Sensing resistors™ a review of the technology," *Electro International, ELECTR 1991 - Conference Record*. pp. 666–668, 1991.

[18] P. Bertemes-Filho and F. Simini, *Bioimpedance in Biomedical Applications and Research*. 2018.

[19] L. Paredes-Madrid, L. Emmi, and P. G. De Santos, "Improving the performance of piezoresistive force sensors by modeling sensor capacitance," *IEEE Int. Symp. Ind. Electron.*, no. August, pp. 458–463, 2010.

[20] L. Paredes-Madrid, L. Emmi, E. Garcia, and P. G. de Santos, "Detailed study of amplitude nonlinearity in piezoresistive force sensors," *Sensors*, vol. 11, no. 9, pp. 8836–8854, 2011.